NEW EVALUATION TECHNIQUE FOR THIN-FILM SOLAR CELL BACK-REFLECTOR USING PHOTOTHERMAL DEFLECTION SPECTROSCOPY

Xunming Deng and K. L. Narasimhan
Energy Conversion Devices, Inc., 1675 West Maple Road, Troy, Michigan 48084

ABSTRACT

We report a new technique to determine the optical loss of a thin-film solar cell back-reflector using Photothermal Deflection Spectroscopy (PDS). We modified a conventional PDS technique to measure the reflection loss of highly reflective and highly textured back reflector surfaces. PDS has demonstrated its advantages in such measurements because, unlike conventional reflectance measurements, it measures the fraction of the light that is converted to heat.

We then used this technique for developing new back-reflectors. We developed a Hot-Ag/Cold-Ag two-layer system in which the texture is provided by the bottom Ag layer deposited at high temperature and low deposition rate, and the reflectance is provided by the top Ag layer deposited at low temperature and high deposition rate. Such a highly reflective and highly textured back-reflector system enhanced the quantum efficiency (QE) of a-Si solar cells both in the red and in the blue regions.

INTRODUCTION

A high performance back-reflector plays an important role in achieving high solar cell efficiency. In particular, for a-Si solar cells deposited on a stainless steel substrate with a structure such as a SS/back-reflector/triple-n-i-p/TCO, a high performance back-reflector must provide both reflectance and surface texture [1]. This type of back-reflector enhances the solar cell efficiency in two ways: 1) the highly reflective surface reflects unabsorbed light back into the solar cell; and 2) the highly textured surface provides efficient light trapping.

In order to further improve back-reflector performance, we need methods to reliably measure its reflection and light trapping capability. The optical loss of a back-reflector is conventionally evaluated by measuring the reflectance using a spectrophotometer equipped with an integrating sphere, and then subtracting the reflectance from the incident light intensity to get the optical loss. However, for a good back-reflector, which is highly reflective and textured, this technique becomes less reliable.

Back-reflector performance is also often evaluated with a complete solar cell device, such as an SS/back-reflector/single n-i-p solar cell/ITO. The long wavelength response in the solar cell quantum efficiency (QE) curve depends sensitively on the back-reflector. A solar cell device is indeed one of the most important tools to evaluate the gain of a back-reflector, however, variation in many parameters, such as the semiconductor layer thickness also strongly affects the solar cell quantum efficiency. Furthermore, it cannot be determined where the optical loss occurs in a complete device from the QE curve measurement.

In this work, we report a new technique to determine the back-reflector optical loss using PDS. Using this technique, we developed a new back-reflector structure with improved texture and reflectance, as will be described.

PDS TECHNIQUE FOR BACK-REFLECTOR EVALUATION

PDS is used extensively in the field of amorphous silicon (a-Si) research for measuring the density of defect states of a-Si thin films [2]. Recently, we modified the PDS technique to evaluate the performance of a solar cell back-reflector deposited on a stainless steel substrate. PDS has proven advantages in the measurement of optical loss, especially for highly reflective and textured surfaces, because (unlike conventional reflectance measurements) PDS measures the fraction of the light that is absorbed and converted to heat.

In a conventional PDS system, monochromatic light is focused on the sample which is immersed in CCl_4 in a cuvette cell. The portion of light that is absorbed by the sample and substrate is converted to heat while the remainder of the light, either transmitted through or reflected back, does not contribute to heat generation. The absorbed light heats up the local region of CCl_4 around the illuminated spot and forms a semisphere of CCl_4 with an increased local temperature and hence a different refractive index. This semisphere acts as a lens, and a HeNe probe beam that passes through the CCl_4 in front of the sample surface is deviated by the CCl_4 lens. A position sensor is then used to detect the shift of the HeNe light spot and the deviation of the light spot on the position sensor is proportional to the amount of heat absorbed by the sample surface. We measure the light intensity of different wavelengths using a thermopile at the position of the sample. Absorption as low as 0.01% can be easily measured by this method.

In current back-reflector research, a back-reflector, such as a textured Ag reflector, is mounted in the cuvette cell. The monochromator light beam is focused onto the back-reflector. With a small portion of the monochromatic light being absorbed by the sample, the majority of the incident light is specularly reflected, or in the case of a textured surface, scattered. The reflected or scattered light does not contribute to the signal that PDS measures since it is not converted into heat inside CCl_4. Therefore, with appropriate calibration, PDS is a powerful tool in measuring

CH3365-4/94/0000-0555 $4.00 © 1994 IEEE

the light absorption loss in highly reflective and highly textured surfaces. Since the back-reflector is reflective over a wide spectrum, we cannot calibrate the PDS absorption measurement using the band-to-band absorption as in the case of a-Si sub-bandgap absorption measurement. Special procedures are therefore followed to achieve reproducibility of PDS signal for different samples.

The output signal we measure includes magnitude and phase information. With every new sample, we adjust the distance between the HeNe laser beam and the sample front surface to maximize the magnitude of the signal. When the PDS signal is maximized, the phase of the signal is always the same for the same type of substrate. The PDS phase is used as an independent check for the signal maximization.

In this new technique, the PDS signal for different wavelengths is calibrated with a Perkin-Elmer 330 Spectrophotometer using plain specular stainless steel (SS). Table 1 lists the PDS signal (V_{pds}) read from the PDS lock-in amplifier and absorption (A) measured with a Perkin-Elmer Spectrophotometer, for a plain stainless steel substrate, as well as the method we used to obtain the calibration factor (C), which is the ratio of absorption (A) to PDS signal (V_{pds}). The calibration factor C in Table 1 was obtained after averaging the measurements for the samples. A plain stainless steel sample is used for the calibration because it is not textured and the absorption is around 30%, which is within the range that the spectrophotometer measures most accurately. When we measure other samples with PDS, we obtain the absorption loss by multiplying V_{pds} with the calibration factor C ($=A/V_{pds}$), which should be the same for all back-reflector samples on stainless steel substrate.

In Table 2, we list the absorption measurement of specular Ag (sample BR13) and the reference sample (BR00) using PDS and using the calibration factor we obtained above. We have identified that the optical loss at 827nm in the reference back-reflector (BR00) is 7.0%. The PDS signal also depends on the substrate. The V_{pds} of the sample on glass is approximately a factor of two higher than the V_{pds} for the same back-reflector sample on stainless steel due to the different thermal constants of the substrate materials.

We routinely check the system reproducibility of the PDS setup by measuring the reference sample BR00. The measurement of this sample has always been reproducible, within a few percent. The absolute PDS signal calibration depends, to some extent, on the surface conditions of the sample to be measured. We are continuing to further our understanding of these conditions in order to calibrate more reliably and accurately.

PDS can also be used to measure the light loss of different solar cell layers without a complete cell structure. In Table 2, we also include the PDS measurements of SS, SS/specular-Ag, SS/textured-Ag/ZnO, SS/specular-Ag/ZnO, SS/specular-Ag/ZnO/n^+ layers.

Besides the optical loss, another important characteristic of a back-reflector is its texture. We complement PDS measurement with 1) the measurement of angular dependence of scattering and 2) a scanning electron microscope. In the angular dependence of scattering measurement, we direct a HeNe laser beam to the back-reflector surface at approximately normal incidence, and measure the light intensity of the specularly reflected light and the scattered light. When the surface is more textured, the percentage of the specularly reflected light will decrease, and the percentage of scattered light at high scattering angle will increase. The texture of the surface is also studied with SEM photographs, taken at 60° electron beam incidence. Such pictures reveal the size and the depth of the texture. We then use these back-reflector evaluation techniques for developing new improved back-reflectors.

DEVELOPMENT OF HOT-Ag/COLD-Ag/ZnO BACK REFLECTOR

The Ag/ZnO back-reflector system that we currently use is highly reflective and textured. When Ag is deposited at high temperature and low deposition rate, it is

Table 1. Calibration of PDS signal with Perkin-Elmer 330 Spectrophotometer using a plain stainless steel sample.

Photon Energy hv(eV)	2.1	1.9	1.7	1.5	1.3	1.1
Wavelength(nm)	590	653	729	827	954	1127
Lock-in output Vpds(mV)	1.32	2.8	4.04	4.69	8.3	9.3
Absorption measured with Perkin-Elmer A	35.5%	34.5%	33.%	31.%	30.%	24.%
Calibration Factor C C=A/Vpds	25.9	12.1	8.4	6.9	3.7	2.6

Table 2. Reflection loss of various layers measured by PDS.

Sample	PDS data	Wavelength(nm)					
		590	653	729	827	954	1127
Stainless Steel (SS)	Vpds(mV)	1.32	2.80	4.04	4.67	8.30	9.30
	Ref'n Loss	34.1%	33.9%	33.9%	32.3%	30.3%	24.4%
SS/Specular-Ag	Vpds(mV)	0.09	0.18	0.23	0.23	0.39	0.41
BR13	Ref'n Loss	2.3%	2.2%	1.9%	1.6%	1.4%	1.1%
SS/Textured-Ag/ZnO	Vpds(mV)	0.57	1.00	1.03	1.00	1.57	1.50
BR00, reference	Vpds(mV)	14.8%	12.1%	8.7%	7.0%	5.7%	3.9%
SS/Specular-Ag/ZnO	Vpds(mV)	0.17	0.40	0.52	0.37	0.67	0.91
	Ref'n Loss	8.5%	4.8%	4.3%	2.6%	2.4%	2.4%
SS/Specular-Ag/ZnO/	Vpds(mV)	1.25	1.82	1.84	1.92	3.22	3.05
/thin n	Ref'n Loss	32.0%	22.0%	15.4%	13.2%	11.8%	8.0%

textured due to the Ag segregation. In order to further enhance the texture and reflectance, we analyze the optical loss using PDS, and analyze the texture using SEM, angular dependence of scattering and solar cell quantum efficiency. An evaporation system is used for exploring the different deposition conditions for the Ag layer. It was found that Ag that is evaporated at high substrate temperature and at low rate is more textured but less reflective, while Ag evaporated at low substrate temperature and at high rate is more reflective but less textured. Table 3 lists the PDS measurement for both Ag evaporated at high temperature (BR12) and at low temperature (BR13).

We have developed a Ag/Ag two-layer system in which the texture and reflectance are achieved by different Ag layers. We utilize the Ag, evaporated at high temperature and low deposition rate (Hot-Ag) to obtain ideal light trapping since the grain size of such Ag is around 0.3-0.4 μm, which is about the same as the wavelength of red light in ZnO, of which the refractive index is 2.0. Because the Ag evaporated at high temperature has relatively lower reflection compared to Ag evaporated at room temperature at high deposition rate (Cold-Ag), we cover the Hot-Ag with a layer of Cold-Ag to form a Ag/Ag double layer structure. In this way, the combined structure (Hot-Ag/Cold-Ag) can provide both efficient reflection and light trapping in solar cells. Table 3 includes the optical loss measured by PDS for a Ag/Ag two-layer system. Although the texture is much improved compared to BR12, as we found from SEM and measurements of the angular dependence of scattering, the reflection loss is smaller than BR12. Fig. 1 shows the SEM picture of a Ag layer deposited at 350°C and a Hot-Ag/Cold-Ag two-layer system.

On the other hand, the reflectance at 827nm for Hot-Ag/Cold-Ag (BR66) is 94.3% while that for specular Ag (BR13) is 98.4%, according to Table 3. It is likely that this slightly reduced reflectance is intrinsic due to the texture. The reflectance of highly specular Ag can be as low as 80% when the incident light is away from normal. For a textured surface, the incident light is microscopically at an angle, resulting in an increased reflection loss.

From Fig. 1 we also find that the size of the texture from Hot-Ag is around 0.4 μm. Therefore, in an SS/Ag/Ag/ZnO/n-i-p/ITO device, the red light is most efficiently scattered and trapped in the device due to the comparable texture size with the wavelength.

To find out whether the reflectance of the Cold-Ag layer degrades when the two-layer back-reflector system is subsequently subjected to high temperature, which it will be during the subsequent ZnO and n-i-p solar cell deposition processes, we annealed the Hot-Ag/Cold-Ag two-layer system at 400°C for 30 min. We observed that the reflectance is not reduced; in fact, it is even slightly improved.

We then deposited an n-i-p solar cell (with i layer thickness of approximately 4000 Å) on the Hot-Ag/Cold-Ag/ZnO back-reflector structure, where approximately 4000 Å of ZnO was deposited using RF sputtering from a ZnO target in a RD Mathis sputtering system. The QE curve of this solar cell is shown in Fig. 2. As a comparison, the QE curve of the same sample on the reference back-reflector, BR00, is also shown in Fig. 2. The J_{ph} from QE for the device on Hot-Ag/Cold-Ag is 17.2 mA/cm^2, while that for the same device on the reference back-reflector is 16.8 mA/cm^2. There are improvements in QE response in both the red and blue regions. The increased red response is due to the reduced reflectance loss and improved light trapping. The increase in the blue response is probably due to the decrease in the reflection loss of the ITO coating when the surface is textured, since 1) normal incident light microscopically enters the ITO at a non-normal incident angle; and 2) the ITO is effectively thinner, which shifts the reflection minimum toward the blue. For this reason, we obtained QE=73% at 400nm for a solar cell deposited on the Hot-Ag/Cold-Ag/ZnO back-reflector, as shown in Fig. 3.

SUMMARY

We have developed a new back-reflector evaluation technique using PDS. This technique is very effective in measuring the optical loss of highly reflective and highly textured surfaces. We used this technique to further improve the back-reflector system. A Hot-Ag/Cold-Ag/ZnO back-reflector system was developed which uses two Ag layers to achieve high texture and high reflectance separately. The improved back-reflector performance is demonstrated in solar cells.

ACKNOWLEDGMENTS

We thank S. R. Ovshinsky, M. Izu, H. Fritzsche, S. Guha, and J. Yang for stimulating and important discussions, and A. Myatt and J. Evans for experimental help. This work was partially supported by DOE/NREL PVMaT 2A Program under subcontract No. ZM-2-11040-7.

REFERENCES

[1] S. Guha, "Research on High-Efficiency, Multiple-Gap, Multi-Junction Amorphous Silicon-Based Alloy Thin-Film Solar Cells", ECD Final Subcontract Report to SERI, under Subcontract ZB-7-06003-4, (1990).

[2] W.B. Jackson, N.M. Amer, A.C. Boccara, and D. Fournier, Appl. Opt. 20, 1333 (1981).

Table 3. PDS measured optical loss at 827 nm for different Ag layers.

Sample	Type		Ts (C)	d (A)	Dep. Rate (A/sec)	PDS data	827nm 1.5eV
BR12	Ag		350	1500	2.0	Vpds(mV)	1.28
						Loss(%)	8.8
BR13	Ag		25	1500	2.0	Vpds(mV)	0.23
						Loss(%)	1.6
BR66	Ag/Ag	top Ag	25	1500	15	Vpds(mV)	0.83
		bottom Ag	400	1000	1.3	Loss(%)	5.7

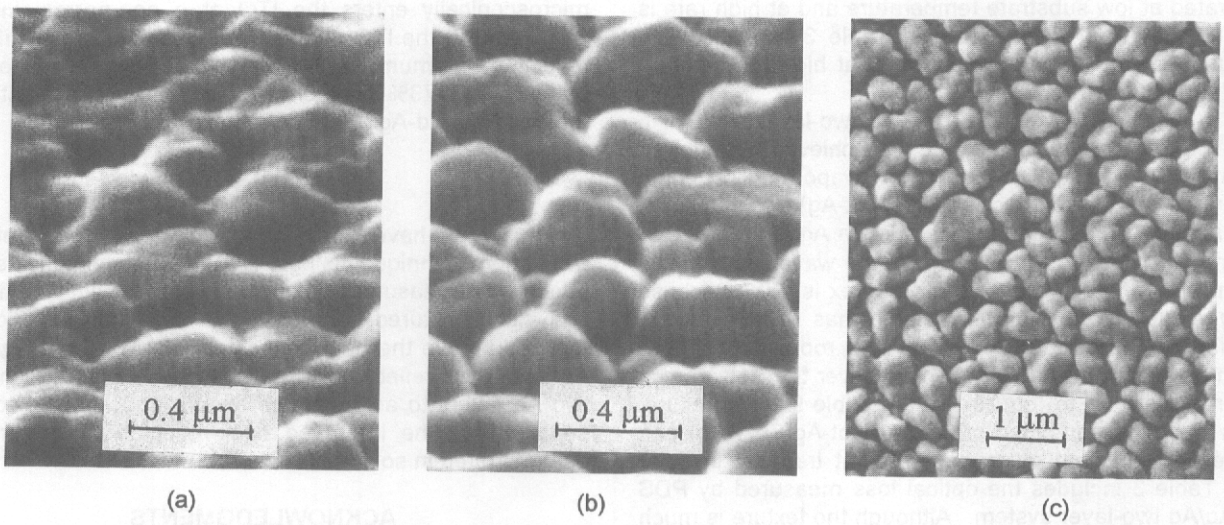

Fig. 1. SEM photographs of different Ag layers. (a) Ag evaporated at 350 C, taken at 60° angle with 40,000x magnification; (b) Hot-Ag/Cold-Ag two layer back-reflector system, taken at 60° angle with 40,000x magnification; and (c) Hot-Ag/Cold-Ag two layer system, taken at normal incidence with 10,000x magnification.

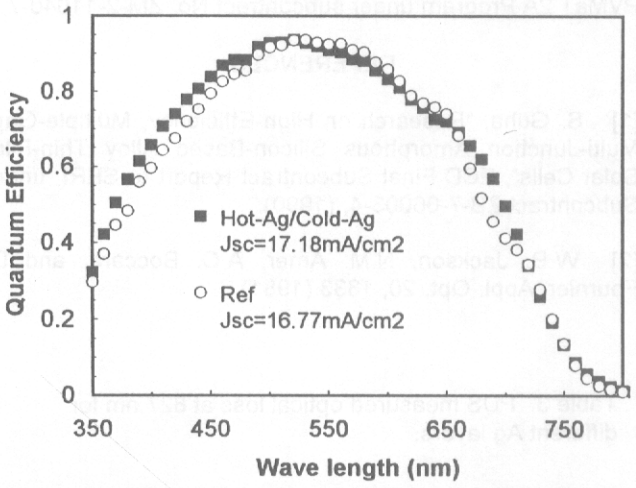

Fig. 2. Quantum efficiency curve of a-Si n-i-p solar cells on the Hot-Ag/Cold-Ag/ZnO back-reflector and on the Ag/ZnO reference back-reflector.

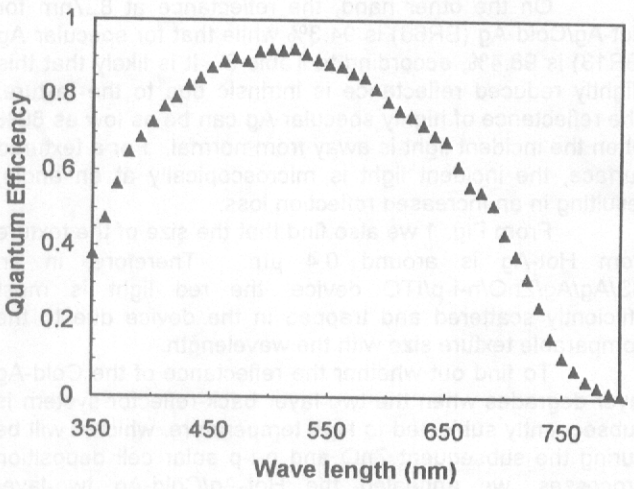

Fig. 3 Quantum efficiency curve of an a-Si n-i-p solar cell with QE=73% at 400 nm.